Table 2. Summary of All the GB Structure Properties[a]

chemical system	supercell stoichiometry	k-points	γ_{GB} (mJ/m^2)	GB density (1/Å)	bulk modulus (GPa)
LiF/LiF (5 GB)	$Li_{112}F_{112}$	5 × 3 × 1	380.79	0.130	76.88
LiF/LiF (3 GB)	$Li_{68}F_{68}$	5 × 4 × 1	423.55	0.136	77.25
Li_2O/Li_2O (3 GB)	$Li_{126}O_{63}$	5 × 5 × 1	688.72	0.166	65.79
Li_2O/Li_2O (5 GB)	$Li_{102}O_{51}$	3 × 4 × 1	557.47	0.118	64.73
LiF/Li_2O	$Li_{120}F_{48}O_{36}$	3 × 3 × 1	288.62	0.124	64.22

[a]The first column shows the GB composition and notation, the second column shows the stoichiometry, the third column lists the k-point mesh used in the present DFT calculations, the fourth column shows the calculated GB energies, the fifth column reports the GB density, and the last sixth column reports the calculated bulk modulus.

Figure 3.(a) Compact LiF/LiF (310) GB (3) with Li adatom (marked in blue). (b) Open LiF/LiF (310) GB (5) with Li adatom (marked in blue). (c) Migration barrier for compact LiF/LiF (310) GB (3). (d) Migration barrier for compact LiF/LiF (310) GB (3).

difference is observed owing to the small sizes of the SEI grain structures. For example, the reported bulk elastic modulus for Li_2O for microscale structures is 56 GPa, whereas the computed value for single-crystal Li_2O (4 nm) is 68 GPa.

Lower values of GB energy, γ_{GB}, indicate a stronger cohesive bonding between the two grains in contact. From the GB energy, γ_{GB}, it can be clearly identified that the Li_2O/Li_2O (3 GB) structure is energetically much less favorable than the Li_2O/Li_2O (15 GB). Furthermore, we also observed that the GB structure breaks apart when we add a Li adatom into this GB.

3.2. Li Diffusion through the GB. In this section, the results of the DFT calculations of Li diffusion through the above identified stable GB are presented. The activation energies (E_{act}) and pre-exponential factors are obtained, and respective diffusion coefficients are calculated. These results are then compared against the available experimental data and other computational results. This provides a better understanding on the interplay between the GBs in the SEI compounds and their effect on direction-dependent ion migration through the GB interface. There are three most common types of Li diffusion mechanisms, that is, hopping, knock-off, and vacancy-assisted diffusion, as identified in the prior literature[24,28,30] and reviewed in the Introduction section. In this work, we mainly observe multiatom hopping mechanism as shown in Figure S3. Because the GB between two adjacent grains creates an opening big enough for Li diffusion, the alternative knock-and vacancy-assisted diffusion should not contribute to a great extent. This is due to the fact that vacancy creation at the most stable surface is energetically not a favorable process. Moreover, Li multiatom coordination inside the GB is a very favorable structure, leading to a more favorable hopping mechanism than any other mechanisms, which involves vacancy formation.

3.2.1. Li Diffusion through LiF/LiF GB. As shown in the previous section, there are two possible GB structures (3 and 5 GB) for LiF/LiF. The migration of a Li atom in the vicinity of the 3 GB and 5 GB and parallel to the GB plane is studied. The simulation cell with the adatom is as shown in Figure 3a,b for 3 GB and 5 GB, respectively.

From the migration barriers as shown in Figure 3c,d, it could be seen that the barrier energy for Li to diffuse through the GB is lower in the case of the open 5 GB than the dense 3 GB. The energy barriers of 0.62 and 1.03 eV for open and dense structures show that the open structure allows for better diffusion through the GB than the dense structure. This might be due to lesser interaction from neighboring atoms in 5 GB.

3.2.2. Li Diffusion through Li_2O/Li_2O GB. This section examines Li diffusion in the simulation cell containing Li_2O crystal with the 15 GB system as shown in Figure 4. In Figure 4a, the simulation cell used for the NEB calculation with the GB and the Li adatom placed at the GB region is shown. From Figure 4b, it could be seen that the migration barrier for Li diffusion through the GB structure is 0.78 eV, which suggests that the diffusion through this GB in Li_2O is slightly more hindered when compared to that of GBs in LiF.

3.2.3. Li Diffusion through LiF/Li_2O GB. This section reports Li diffusion in the simulation cell containing Li_2O Li

DOI: 10.1021/acs.jpcc.9b00436
J. Phys. Chem. C 2019, 123, 10235−10245

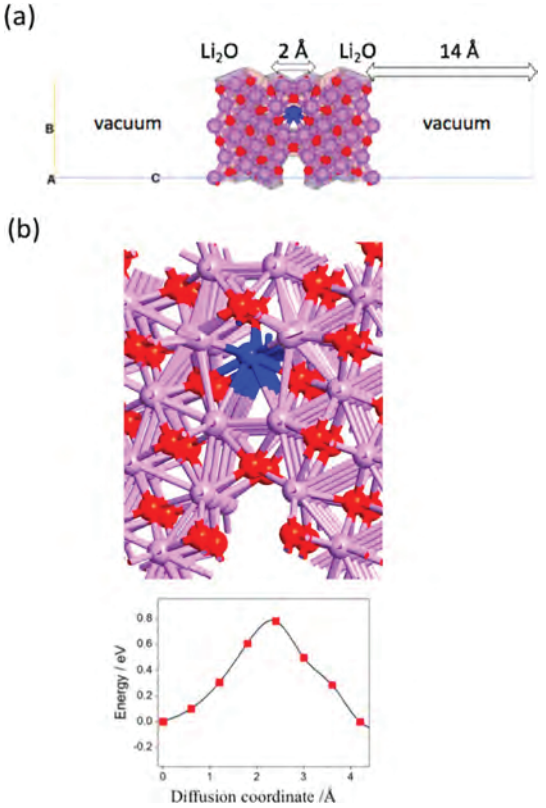

Figure 4. (a) Li_2O/Li_2O (210) GB (Σ15) with Li adatom (marked in blue). (b) Diffusion direction and migration barrier for Li_2O/Li_2O (310) GB (Σ15).

crystal on one side and LiF on the other with a GB interface. The migration of a Li atom in the vicinity of the GB and parallel to the GB plane is studied. However, unlike the case of LiF/LiF GBs or Li_2O/Li_2O GBs, in this structure there are different channels that could act as possible MEPs for Li diffusion. From Figure 5b–d, it could be seen that the migration barrier for Li diffusion through the GB structure ranges between 0.45 and 1 eV in the three paths and the MEP is as shown in Figure 5c and the migration barrier is 0.45 eV.

On the basis of all the evaluated values of migration barriers, the diffusion coefficients through all the GB systems are calculated and listed in Table 3. According to the results

Table 3. Summary of All Activation Energies and Diffusion Coefficients for Li Diffusion in the Respective GB

GB configuration	activation energy (eV)	pre-exponential factor (m^2/s)	diffusion coefficient (m^2/s)
LiF/LiF (Σ5 GB)	0.68	1.76×10^{-6}	4.6×10^{-16}
LiF/LiF (Σ3 GB)	1.03	1.23×10^{-6}	3.16×10^{-23}
Li_2O/Li_2O (Σ15 GB)	0.78	3.70×10^{-6}	7.38×10^{-16}
LiF/Li_2O	0.45	1.59×10^{-6}	3.87×10^{-14}

presented in Table 3, Li diffusion through the LiF/Li_2O GB is the most favorable mechanism because of the low energy barrier and a short diffusion distance. Physically, it occurs because of a multiatom hoping mechanism as discussed above. In this mechanism, Li is bonded to several different atoms while diffusing across the GB, which makes the diffusion process fast. It should be noted that the diffusion coefficients are calculated based on the Arrhenius equation (eq 3) assuming the attempt frequency of the first-order reaction (the order of the Debye frequency). In addition, the tracer correlation factor is set to one for simplicity. All of these factors

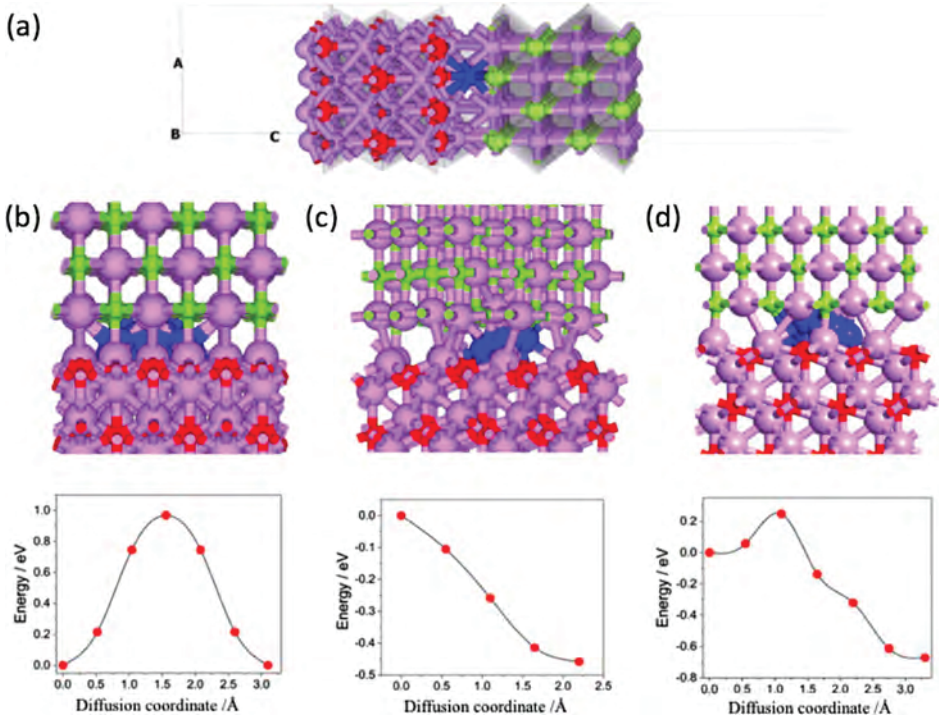

Figure 5. (a) LiF/Li_2O GB with Li adatom (marked in blue). (b) Diffusion direction (path 1) and migration barrier for LiF/Li_2O GB. (c) Diffusion direction (path 2) and migration barrier for LiF/Li_2O GB. (d) Diffusion direction (path 3) and migration barrier for LiF/Li_2O GB.

DOI: 10.1021/acs.jpcc.9b00436
J. Phys. Chem. C 2019, 123, 10237−10245

could potentially alter the diffusion coefficient values of Li in the GB. The diffusion dimensionality in each GB system is different. In the case of LiF/LiF GBs (both Σ5 and Σ3), the dimensionality of Li diffusion is 1 owing to the straight path of diffusion, whereas in the case of Li_2O/Li_2O GB, it is 2 and for LiF/Li_2O, it is 2 or 3 depending on the path.

Putting together the information regarding individual components in the SEI provides us an improved overall picture of transport through these complex interphases and their connection to the battery performance. Thus, we further compare our calculated energy barriers and the diffusion coefficients with those taken from the prior literature. In particular, we compare Li diffusion through the GB with the corresponding diffusion rate in the single components, which create the GB.

In the work of Chen et al.[31] the calculated Li migration energy barriers from DFT, along the major diffusion pathways of the three main components, LiF, Li_2O, and Li_2CO_3, were 0.73 eV, 0.152−1.362 eV, and 0.227−0.491 eV, respectively. Similar results for the energy barrier were found in the other DFT studies, where the lithium dynamics through LiF is investigated.[24,54] One of the most reported inorganic components that is found in the SEI is LiF.[24,25,31,54,55] Yildrim et al.[24] reported that the positively charged ion diffusivity in LiF is much lower than that in the other SEI inorganic components and suggested that diffusion in LiF is very slow, causing rate limitations in Li-ion diffusion. They used the DFT calculations to determine diffusion pathways and NEB method to calculate energy barriers of diffusion. They found that in the bulk of LiF, diffusion of vacancies is energetically more favorable than interstitials, and reported energy barriers of 0.73 and 1.09 eV for neutral vacancies and neutral Schottky vacancies, respectively, and the associated diffusion coefficients were reported in the order of 10^{-26} to -10^{-20} m^2/s. Recent studies, using the phase-field model together with Fick's law,[56] report a diffusion coefficient of Li in LiF at room temperatures (298−318 K) in the range of 3.7×10^{-16} m^2/s. Through our current DFT study with the GB structures of LiF, we determine that the migration energy barrier for Li-ion diffusion through the GB structure was 0.68 eV for Σ5 GB and 1.03 eV for Σ3 GB, which corresponds to diffusion coefficients of 4.60×10^{-16} m^2/s and 3.16×10^{-23} m^2/s, respectively. The diffusion coefficient values fall within the range of 10^{-26} to -10^{-16} m^2/s, which have been reported in different phase-field, molecular dynamics and NEB methods for the diffusion of Li in LiF. Considering the broad range of diffusion coefficients reported in the prior literature, we can conclude that our results indicate that Li diffusion through the LiF/LiF GB is faster or comparable to that of a pure grain.

In the case of Li_2O, only a very few theoretical studies reported the diffusion barriers through their bulk structures at low temperature.[31,57] Tasaki et al.[55] studied the diffusion of Li_2O and found transport coefficients in the range of 1.7×10^{-16} m^2/s. The current DFT results as shown in Table 3 suggest that the diffusion through the Li_2O/Li_2O GB system is at least 1 order of magnitude faster than that of the bulk structures of Li_2O.

There are no existing theoretical studies to compare the polycrystalline GB system that is considered in our current study. However, on comparing the values of diffusion coefficients obtained for the LiF/Li_2O GB system against the bulk LiF and the bulk Li_2O from the prior literature, we can see that there is a significant increase in the diffusion coefficient for the diffusion through the LiF/Li_2O GB system forming the rate-determining step in the diffusion process.

Experimentally, it is reported that the activation energy for lithium diffusion in the SEI ranges from 0.37 to 0.67 eV.[58−60] However, this value is very sensitive toward factors such as the charge/discharge state, the operating temperature, the content of the electrolyte, and so forth.[58,59] Therefore, quantitative comparison of the experimental data with our calculated energy barrier is not possible. However, qualitatively, our data are in good agreement with the experimental findings. Furthermore, as the energy barrier for lithium diffusion in LiF is substantially higher than in Li_2CO_3 and Li_2O, it is reasonable to conclude that the low lithium electrodeposited amount could be a side evidence of more LiF in the SEI when other conditions are similar.

Because the rate-determining step in the diffusion process is the diffusion through the GB, sub nanometer-sized particles of the Li metal can grow in these atomic length scale gaps in the GB, resulting in the nucleation of lithium filaments that may cause subsequent growth of dendrites under adverse conditions. This observation is also consistent with the fact that applying pressure or a mechanical barrier reduces the void spaces and improves the performance of Li metal anodes.[61]

4. SUMMARY AND CONCLUSIONS

The SEI growth rate, structure, composition, and resistance significantly depend upon the electrolyte composition. Furthermore, the distribution of intercalated/electrodeposited Li greatly depends on the SEI structure, which defines the subsequent electric potential gradient and the stress field.[62] Thus, the understanding of the Li diffusion mechanism and its energetics through the SEI is of imperative importance to understand and improve the performance of Li batteries. For that reason, in this work, we employ the first-principles calculations based on DFT to investigate different aspects of Li atom diffusion through the GB of the SEI. In this work, we consider the most studied, however, not greatly understood SEI of LIBs and LMBs. In particular, five different GB structures are investigated, and their interface atomic and electronic structures are carefully analyzed. It is revealed that the LiF/LiF, Li_2O/Li_2O, and LiF/Li_2O GBs are the most stable configurations. Subsequently, the Li diffusion mechanism and energetics through these stable GB interfaces are investigated. Among the studied GBs, the fastest Li diffusion rate is observed for the heterogeneous LiF/Li_2O GB, compared to the homogeneous LiF/LiF and Li_2O/Li_2O. This is due to the fact that Li multiatom coordination inside the GB is a very favorable structure, leading to the multiatom hopping mechanism that is more advantageous than any other mechanisms.

Because little is known about the actual structure and configuration of the GB in the SEI of operating cells, the presently investigated GB for the Li diffusion might be simpler than the real-cell structures. For example, numerous defects and/or impurities could exist in the local structure of the SEI, which could potentially influence Li diffusivity. In addition, there are other external factors that could influence Li diffusivity in the SEI, such as an applied electric field and temperature.[58] However, it is expected that these external factors would influence Li diffusion through the GB in the same way as through the respective grains.

Nevertheless, the relatively low DFT computational cost using the GB configuration of 200−300 atoms enables a broad

DOI: 10.1021/acs.jpcc.9b00436
J. Phys. Chem. C 2019, 123, 10237−10245

range of parametric studies that could suggest new and/or improved strategies for Li dendrite formation and growth in the case of LMBs. Moreover, it is common in the higher hierarchy cell-level models to represent the SEI as a constant resistance ignoring its chemistry and transport properties. However, incorporating the details of the ion diffusion and the detailed SEI chemistry into battery cell-level models, in a more fundamental manner, could enable the profound investigation of the SEI influence on battery performance and efficiency. Thus, the results from the present work, in addition to revealing the diffusion mechanism of Li in the GB of the SEI, are a step forward toward more robust cell models.

■ ASSOCIATED CONTENT

Supporting Information

The Supporting Information is available free of charge on the ACS Publications website at DOI: 10.1021/acs.jpcc.9b00436.

Details of the bulk crystal structure, minimum energy surface slabs, and hopping mechanism of Li diffusion through the GB structures (PDF)

■ AUTHOR INFORMATION

Corresponding Author

*E-mail: mashayek@uic.edu. Phone: +1 (312) 996 1154.

ORCID

Ajaykrishna Ramasubramanian: 0000-0003-3005-6665

Vitaliy Yurkiv: 0000-0002-3407-891X

Tara Foroozan: 0000-0003-1334-3048

Reza Shahbazian-Yassar: 0000-0002-7744-4780

Notes

The authors declare no competing financial interest.

■ ACKNOWLEDGMENTS

The authors acknowledge the financial support from the National Science Foundation award CBET-1805938. In addition, the authors would like to acknowledge the Advanced Cyberinfrastructure for Education and Research (ACER) group at The University of Illinois at Chicago (URL: https://acer.uic.edu) as well as the National Science Foundation Extreme Science and Engineering Discovery Environment (XSEDE) award no. TG-DMR180106 for providing HPC resources that have contributed to the research results reported in this paper.

■ REFERENCES

(1) Scrosati, B.; Hassoun, J.; Sun, Y.-K. Lithium-Ion Batteries. A Look into the Future. *Energy Environ. Sci.* **2011**, *4*, 3287−3295.

(2) Thackeray, M. M.; Wolverton, C.; Isaacs, E. D. Electrical Energy Storage for Transportation− Approaching the Limits of, and Going Beyond, Lithium-Ion Batteries. *Energy Environ. Sci.* **2012**, *5*, 7854−7863.

(3) Yu, X.; Manthiram, A. Electrode-Electrolyte Interfaces in Lithium-Based Batteries. *Energy Environ. Sci.* **2018**, *11*, 527−543.

(4) Cheng, X.-B.; Zhang, R.; Zhao, C.-Z.; Wei, F.; Zhang, J.-G.; Zhang, Q. A Review of Solid Electrolyte Interphases on Lithium Metal Anode. *Adv. Sci.* **2015**, *3*, 1500213.

(5) Yan, C.; Cheng, X.-B.; Zhao, C.-Z.; Huang, J.-Q.; Yang, S.-T.; Zhang, Q. Lithium Metal Protection through in Situ Formed Solid Electrolyte Interphase in Lithium-Sulfur Batteries: The Role of Polysulfides on Lithium Anode. *J. Power Sources* **2016**, *327*, 212−220.

(6) Yurkiv, V.; Foroozan, T.; Ramasubramanian, A.; Shahbazian-Yassar, R.; Mashayek, F. Phase-Field Modeling of Solid Electrolyte Interface (SEI) Influence on Li Dendritic Behavior. *Electrochim. Acta* **2018**, *265*, 609−619.

(7) Peled, E. The Electrochemical Behavior of Alkali and Alkaline Earth Metals in Nonaqueous Battery Systems-The Solid Electrolyte Interphase Model. *J. Electrochem. Soc.* **1979**, *126*, 2047−2051.

(8) Peled, E.; Golodnttsky, D.; Ardel, G.; Menachem, C.; Bar Tow, D.; Eshkenazy, V. The Role of Sei in Lithium and Lithium Ion Batteries. *MRS Proc* **1995**, *393*, 209−219.

(9) Peled, E.; Menachem, C.; Bar Tow, D.; Melman, A. Improved Graphite Anode for Lithium-Ion Batteries Chemically. *J. Electrochem. Soc.* **1996**, *143*, L4−L7.

(10) Peled, E.; Golodnitsky, D.; Ardel, G. Advanced Model for Solid Electrolyte Interphase Electrodes in Liquid and Polymer Electrolytes. *J. Electrochem. Soc.* **1997**, *144*, L208−L210.

(11) Broussely, M.; Biensan, P.; Bonhomme, F.; Blanchard, P.; Herreyre, S.; Nechev, K.; Staniewicz, R. J. Main Aging Mechanisms in Li Ion Batteries. *J. Power Sources* **2005**, *146*, 90−96.

(12) Vetter, J.; Novák, P.; Wagner, M. R.; Veit, C.; Möller, K.-C.; Besenhard, J. O.; Winter, M.; Wohlfahrt-Mehrens, M.; Vogler, C.; Hammouche, A. Ageing Mechanisms in Lithium-Ion Batteries. *J. Power Sources* **2005**, *147*, 269−281.

(13) Zhang, H.-L.; Li, F.; Liu, C.; Tan, J.; Cheng, H.-M. New Insight into the Solid Electrolyte Interphase with Use of a Focused Ion Beam. *J. Phys. Chem. B* **2005**, *109*, 22205−22211.

(14) Verma, P.; Maire, P.; Novák, P. Electrochimica Acta Review Article A Review of the Features and Analyses of the Solid Electrolyte Interphase in Li-Ion Batteries. *Electrochim. Acta* **2010**, *55*, 6332−6341.

(15) Smith, A. J.; Burns, J. C.; Zhao, X.; Xiong, D.; Dahn, J. R. A High Precision Coulometry Study of the SEI Growth in Li/graphite Cells. *J. Electrochem. Soc.* **2011**, *158*, A447−A452.

(16) Edström, K.; Herstedt, M.; Abraham, D. P. A New Look at the Solid Electrolyte Interphase on Graphite Anodes in Li-Ion Batteries. *J. Power Sources* **2006**, *153*, 380−384.

(17) Lu, M.; Cheng, H.; Yang, Y. A Comparison of Solid Electrolyte Interphase (SEI) on the Artificial Graphite Anode of the Aged and Cycled Commercial Lithium Ion Cells. *Electrochim. Acta* **2008**, *53*, 3539−3546.

(18) Cresce, A. V.; Russell, S. M.; Baker, D. R.; Gaskell, K. J.; Xu, K. In Situ and Quantitative Characterization of Solid Electrolyte Interphases. *Nano Lett.* **2014**, *14*, 1405−1412.

(19) Shi, S.; Lu, P.; Liu, Z.; Qi, Y.; Hector, L. G.; Li, H.; Harris, S. J. Direct Calculation of Li-Ion Transport in the Solid Electrolyte Interphase. *J. Am. Chem. Soc.* **2012**, *134*, 15476−15487.

(20) Aurbach, D.; Markovsky, B.; Levi, M. D.; Levi, E.; Schechter, A.; Moshkovich, M.; Cohen, Y. New Insights into the Interactions between Electrode Materials and Electrolyte Solutions for Advanced Nonaqueous Batteries. *J. Power Sources* **1999**, *81-82*, 95−111.

(21) Wang, A.; Kadam, S.; Li, H.; Shi, S.; Qi, Y. Review on Modeling of the Anode Solid Electrolyte Interphase (SEI) for Lithium-Ion Batteries. *npj Comput. Mater.* **2018**, *4*, 15.

(22) Tarascon, J.-M.; Armand, M. Issues and Challenges Facing Rechargeable Lithium Batteries. *Nature* **2001**, *414*, 359−367.

(23) Shi, S.; Gao, J.; Liu, Y.; Zhao, Y.; Wu, Q.; Ju, W.; Ouyang, C.; Xiao, R. Multi-Scale Computation Methods: Their Applications in Lithium-Ion Battery Research and Development. *Chin. Phys. B* **2016**, *25*, 018212.

(24) Yildirim, H.; Kinaci, A.; Chan, M. K. Y.; Greeley, J. P. First-Principles Analysis of Defect Thermodynamics and Ion Transport in Inorganic SEI Compounds : LiF and NaF. *ACS Appl. Mater. Interfaces* **2015**, *7*, 18985−18996.

(25) Liu, Z.; Qi, Y.; Lin, Y. X.; Chen, L.; Lu, P.; Chen, L. Q. Interfacial Study on Solid Electrolyte Interphase at Li Metal Anode: Implication for Li Dendrite Growth. *J. Electrochem. Soc.* **2016**, *163*, A592−A598.

(26) Shi, S.; Zhang, H.; Ke, X.; Ouyang, C.; Lei, M.; Chen, L. First-Principles Study of Lattice Dynamics of $LiFePO_4$. *Phys. Lett. A* **2009**, *373*, 4096−4100.

(27) Zhao, Q.; Pan, L.; Li, Y.-J.; Chen, L.-Q.; Shi, S.-Q. Rotational Motion of Polyanion versus Volume Effect Associated with Ionic

Conductivity of Several Solid Electrolytes. *Rare Met.* **2018**, *37*, 497−503.
(28) Benitez, L.; Cristancho, D.; Seminario, J. M.; Martinez de la Hoz, J. M.; Balbuena, P. B.; Tarascon, J. M.; Armand, M. Electron Transfer through Solid-Electrolyte-Interphase Layers Formed on Si Anodes of Li-Ion Batteries. *Electrochim. Acta* **2014**, *140*, 250−257.
(29) Shi, S.; Qi, Y.; Li, H.; Hector, L. G. Defect Thermodynamics and Diffusion Mechanisms in Li_2CO_3 and Implications for the Solid Electrolyte Interphase in Li-Ion Batteries. *J. Phys. Chem. C* **2013**, *117*, 8579−8593.
(30) Soto, F. A.; Marzouk, A.; El-Mellouhi, F.; Balbuena, P. B. Understanding Ionic Diffusion through SEI Components for Lithium-Ion and Sodium-Ion Batteries: Insights from First-Principles Calculations. *Chem. Mater.* **2018**, *30*, 3315−3322.
(31) Chen, Y. C.; Ouyang, C. Y.; Song, L. J.; Sun, Z. L. Electrical and Lithium Ion Dynamics in Three Main Components of Solid Electrolyte Interphase from Density Functional Theory Study. *J. Phys. Chem. C* **2011**, *115*, 7044−7049.
(32) Christensen, J.; Newman, J. A Mathematical Model for the Lithium-Ion Negative Electrode Solid Electrolyte Interphase. *J. Electrochem. Soc.* **2004**, *151*, A1977−A1988.
(33) Leung, K.; Jungjohann, K. L. Spatial Heterogeneities and Onset of Passivation Breakdown at Lithium Anode Interfaces. *J. Phys. Chem. C* **2017**, *121*, 20188−20196.
(34) Kresse, G.; Furthmüller, J. Efficient iterative schemes forab initiototal-energy calculations using a plane-wave basis set. *Phys. Rev. B: Condens. Matter Mater. Phys.* **1996**, *54*, 11169−11186.
(35) Blöchl, P. E. Projector Augmented-Wave Method. *Phys. Rev. B: Condens. Matter Mater. Phys.* **1994**, *50*, 17953−17979.
(36) Perdew, J. P.; Ruzsinszky, A.; Csonka, G. I.; Vydrov, O. A.; Scuseria, G. E.; Constantin, L. A.; Zhou, X.; Burke, K. Restoring the Density-Gradient Expansion for Exchange in Solids and Surfaces. *Phys. Rev. Lett.* **2008**, *100*, 136406−136411.
(37) Perdew, J. P.; Burke, K.; Ernzerhof, M. Generalized Gradient Approximation Made Simple. *Phys. Rev. Lett.* **1996**, *77*, 3865−3868.
(38) Henkelman, G.; Uberuaga, B. P.; Jónsson, H.; Henkelman, G. A Climbing Image Nudged Elastic Band Method for Finding Saddle Points and Minimum Energy Paths. *J. Chem. Phys.* **2000**, *113*, 9901.
(39) Mouhat, F.; Coudert, F. X. Necessary and Sufficient Elastic Stability Conditions in Various Crystal Systems. *Phys. Rev. B: Condens. Matter Mater. Phys.* **2014**, *90*, 224104.
(40) Lenchuk, O.; Rohrer, J.; Albe, K. Cohesive Strength of Zirconia/molybdenum Interfaces and Grain Boundaries in Molybdenum: A Comparative Study. *Acta Mater.* **2017**, *135*, 150−157.
(41) Yu, R.; Zhu, J.; Ye, H. Q. Calculations of Single-Crystal Elastic Constants Made Simple. *Comput. Phys. Commun.* **2010**, *181*, 671−675.
(42) Panahian Jand, S.; Kaghazchi, P. The Role of Electrostatic Effects in Determining the Structure of LiF-Graphene Interfaces. *J. Phys.: Condens. Matter* **2014**, *26*, 262001.
(43) Radin, M. D.; Rodriguez, J. F.; Tian, F.; Siegel, D. J. Lithium Peroxide Surfaces Are Metallic, While Lithium Oxide Surfaces Are Not. *J. Am. Chem. Soc.* **2012**, *134*, 1093−1103.
(44) Bruno, M.; Prencipe, M. Ab initio quantum-mechanical modeling of the (001), and (110) surfaces of zabuyelite (Li2CO3). *Surf. Sci.* **2007**, *601*, 3012−3019.
(45) Nie, M.; Chalasani, D.; Abraham, D. P.; Chen, Y.; Bose, A.; Lucht, B. L. Lithium Ion Battery Graphite Solid Electrolyte Interphase Revealed by Microscopy and Spectroscopy. *J. Phys. Chem. C* **2013**, *117*, 1257−1267.
(46) Nie, M.; Abraham, D. P.; Chen, Y.; Bose, A.; Lucht, B. L. Silicon Solid Electrolyte Interphase (SEI) of Lithium Ion Battery Characterized by Microscopy and Spectroscopy. *J. Phys. Chem. C* **2013**, *117*, 13403−13412.
(47) Parimalam, B. S.; MacIntosh, A. D.; Kadam, R.; Lucht, B. L. Decomposition Reactions of Anode Solid Electrolyte Interphase (SEI) Components with LiPF6. *J. Phys. Chem. C* **2017**, *121*, 22733−22738.
(48) Santoro, A.; Mighell, A. D. Coincidence-site lattices. *Acta Crystallogr., Sect. A: Cryst. Phys., Diffr., Theor. Gen. Crystallogr.* **1973**, *29*, 169−175.
(49) *Atomistix Toolkit*, version 2016.4; Synopsys QuantumWise A/S, 2016.
(50) Stradi, D.; Jelver, L.; Smidstrup, S.; Stokbro, K. Method for Determining Optimal Supercell Representation of Interfaces. *J. Phys.: Condens. Matter* **2017**, *29*, 185901.
(51) Schneider, J.; Hamaekers, J.; Chill, S. T.; Smidstrup, S.; Bulin, J.; Thesen, R.; Blom, A.; Stokbro, K. ATK-ForceField: a new generation molecular dynamics software package. *Modell. Simul. Mater. Sci. Eng.* **2017**, *25*, 085007.
(52) Smidstrup, S.; Pedersen, A.; Stokbro, K.; Jónsson, H. Improved Initial Guess for Minimum Energy Path Calculations. *J. Chem. Phys.* **2014**, *140*, 214106.
(53) Kim, H.; Windl, W. Efficient Ab-Initio Calculation of the Elastic Properties of Nanocrystalline Silicon. *J. Comput. Theor. Nanosci.* **2007**, *4*, 65−70.
(54) Fan, L.; Zhuang, H. L.; Gao, L.; Lu, Y.; Archer, L. A. Regulating Li Deposition at Artificial Solid Electrolyte Interphases. *J. Mater. Chem. A* **2017**, *5*, 3483−3492.
(55) Tasaki, K.; Goldberg, A.; Lian, J.; Walker, M.; Timmons, A.; Harris, S. J. Solubility of Lithium Salts Formed on the Lithium-Ion Battery Negative Electrode Surface in Organic Solvents. *J. Electrochem. Soc.* **2009**, *156*, A1019−A1027.
(56) Guan, P.; Liu, L.; Lin, X. Simulation and Experiment on Solid Electrolyte Interphase (SEI) Morphology Evolution and Lithium-Ion Diffusion. *J. Electrochem. Soc.* **2015**, *162*, A1798−A1808.
(57) Koyama, Y.; Yamada, Y.; Tanaka, I.; Nishitani, S. n. R.; Adachi, H.; Murayama, M.; Kanno, R. Evaluation of Migration Energy of Lithium Ions in Chalcogenides and Halides by First Principles Calculation. *Mater. Trans.* **2002**, *43*, 1460−1463.
(58) Churikov, A. V. Transfer Mechanism in Solid-Electrolyte Layers on Lithium: Influence of Temperature and Polarization. *Electrochim. Acta* **2001**, *46*, 2415−2426.
(59) Levi, M. D.; Wang, C.; Aurbach, D. Self-Discharge of Graphite Electrodes at Elevated Temperatures Studied by CV and Electrochemical Impedance Spectroscopy. *J. Electrochem. Soc.* **2004**, *151*, A781−A790.
(60) Schranzhofer, H.; Bugajski, J.; Santner, H. J.; Korepp, C.; Möller, K.-C.; Besenhard, J. O.; Winter, M.; Sitte, W. Electrochemical Impedance Spectroscopy Study of the SEI Formation on Graphite and Metal Electrodes. *J. Power Sources* **2006**, *153*, 391−395.
(61) Mikhaylik, Y. V.; Kovalev, I.; Schock, R.; Kumaresan, K.; Xu, J.; Affinito, J. High Energy Rechargeable Li-S Cells for EV Application: Status, Remaining Problems and Solutions. *ECS Trans.* **2009**, *25*, 23−34.
(62) Yurkiv, V.; Foroozan, T.; Ramasubramanian, A.; Shahbazian-Yassar, R.; Mashayek, F. The Influence of Stress Field on Li Electrodeposition in Li-Metal Battery. *MRS Commun.* **2018**, *8*, 1285−1291.

DOI: 10.1021/acs.jpcc.9b00436
J. Phys. Chem. C 2019, 123, 10237−10245